Since January 2020 Elsevier has created a COVID-19 resource centre with free information in English and Mandarin on the novel coronavirus COVID-19. The COVID-19 resource centre is hosted on Elsevier Connect, the company's public news and information website.

VIROLOGY 207, 316–320 (1995)

SHORT COMMUNICATION

Identification and Characterization of a 65-kDa Protein Processed from the Gene 1 Polyprotein of the Murine Coronavirus MHV-A59

MARK R. DENISON,*,[1] SCOTT A. HUGHES,† and SUSAN R. WEISS†

*Department of Pediatrics and Microbiology & Immunology and the Elizabeth B. Lamb Center for Pediatric Research, Vanderbilt University, Nashville, Tennessee 37232-2581; and †Department of Microbiology, University of Pennsylvania Medical School, Philadelphia, Pennsylvania, 19104

Received September 21, 1994; accepted November 18, 1994

A 65-kDa protein has been detected in mouse hepatitis virus A59 (MHV-A59)-infected DBT cells using polyclonal antibodies directed against polypeptides encoded by the 5′ 1.8 kb of gene 1. The presence of this 65-kDa protein (p65) was previously predicted from immunoprecipitation studies of gene 1 expression in MHV-A59-infected DBT cells with other antisera (*1*). p65 was rapidly labeled in virus-infected cells at late times of infection; however, its cleavage from the polyprotein was significantly delayed compared to the amino-terminal gene 1 polyprotein cleavage product, p28. Similar to p28, p65 was cleaved from the growing polyprotein without detectable intermediate precursors. Kinetic analysis of p65 with specific antibodies indicates that p65 is immediately adjacent to p28 in the gene 1 polyprotein. The proteolytic activity responsible for the carboxy-terminal cleavage of p65, as well as the function of the p65 protein, remains to be determined.

Gene 1 of MHV-A59 is 21,798 nt in length and contains two overlapping open reading frames, ORFs 1a and 1b, connected by a functional ribosomal frameshift. Together ORFs 1a and 1b are predicted to encode a polyprotein of approximately 750 kDa. Gene 1 has been shown to encode at least one proteinase and is predicted to encode two additional proteinases, as well as polymerase, helicase, and metal binding zinc finger proteins (*2–6*). Gene 1 translation products have been detected both in virus-infected DBT cells and during *in vitro* translation of purified virion RNA and synthetic RNA transcripts (*7–10*). We have previously identified and characterized the translation and processing of several intracellular gene 1 ORF 1a products including p28, p290, p50, and p240 (*1*). Based on the processing pattern and the known locations of polypeptides used to encode antibodies for that study, we predicted an additional protein immediately adjacent to the amino-terminal p28 protein. To determine whether in fact such a protein was present, an additional antiserum was generated to allow detection of any proteins encoded by the first 1.8 kb of gene 1 ORF 1a, including p28 and adjacent proteins. We describe here the kinetics of expression and processing of a 65-kDa protein cleavage product from the MHV-A59 ORF 1a polyprotein in virus-infected cells.

[1] To whom reprint requests should be addressed: Fax: (615) 343-9723; email: denison@ctrvax.vanderbilt.edu.

The previously determined pattern of gene 1 expression is shown in Fig. 1. A new antiserum, designated UP102, was induced in rabbits against a 60-kDa fusion protein expressed in *Escherichia coli* from a PET plasmid containing a cDNA from nucleotides 180 to 1984 in gene 1 ORF 1a (*11, 12*). This clone extends beyond the coding region of p28 by approximately 1 kb and is predicted by computer analysis of the gene 1 coding sequence to contain several antigenic epitopes in the region of the fusion protein downstream from p28 (*13*). This antibody was used in conjunction with the previously described 81043 polyclonal antiserum to identify additional proteins encoded in the first 3 kb of ORF 1a. The antibodies were used to immunoprecipitate [^{35}S]methionine-labeled viral proteins in DBT cells. The length of infection and time of labeling were based on previous observations concerning maximal detection of ORF 1a gene products during MHV-A59 infection of DBT cells (*1*).

We first performed pulse-labeling experiments with and without synchronization of translation by high salt (Fig. 2). We detected the previously identified p28 protein by 30 min after addition of [^{35}S]methionine, in both synchronized and nonsynchronized pulse-labeling experiments (*14, 1*). p28 was the first protein detected, and no precursors were identified, consistent with previous results. UP102 also immunoprecipitated distinct products of 65 and 180 kDa, as well as a heterogeneous band of protein migrating at the top of the 5–18% gradient gel

0042-6822/95 $6.00

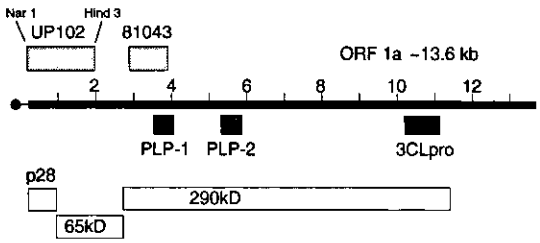

FIG. 1. Antibody location, predicted functional domains, and translation products of MHV-A59 ORF 1a. The bold line indicates the ~13.6 kb of gene 1 ORF 1a, with the coding sequence beginning at the AUG at nt 210 and presumably ending in the heptanucleotide sequence terminating at nt 13,598. Black boxes beneath the line are the regions incorporating known (PLP-1) or predicted (PLP-2 and 3CLpro) proteinases. PLP-1 and PLP-2 indicate papain-like proteinases and 3CLpro indicates the 3C-like proteinase. The exact coding sequences of these proteinases have not been determined. The shaded boxes above the line are the coding regions used to produce fusion proteins for induction of polyclonal rabbit 81043 and UP102 antisera. UP102 was induced against a fusion protein encoding the region of gene 1 from the *Nar*I site at nt 180 to the *Hind*III site at nt 1984. The white boxes below the line identify products of ORF 1a translation in virus-infected cells; the exact amino-termini and coding sequences of these proteins have not been determined.

(*12, 15*). The 180-kDa band was seen only in virus-infected cells but was precipitated by preimmune serum, indicating nonspecific binding of a viral protein or a cellular protein induced in virus-infected cells. The nonspecific nature of the binding of the 180-kDa protein is supported by the fact that it is has been detected by every antiserum used to date, including those raised against proteins encoded at the C-terminus of ORF 1b (*1*). Utilizing limited proteolysis digests, the 180-kDa protein has previously been identified as the S glycoprotein (*1*). Radiolabeled products migrating at the top of the gel have been difficult to size accurately but are definitely larger than 400 kDA. Inability to detect these large products in mock-infected cells or in virus-infected cells immunoprecipitated with preimmune serum suggests that they are specific viral proteins containing epitopes recognized by UP102. Finally, a faint band with a migration of ~250 kDa is intermittently detected with both UP102 and 81043. Because a band of similar migration is sometimes observed in mock-infected cells and occasionally by preimmune sera, it is more likely to be a nonspecific product than an authentic ORF 1a precursor. However, because of the challenges of protein sizing in this region, as well as the presence of several proteins, we cannot entirely rule out that this protein is part of an alternative processing pathway, such as those seen in the processing of the poliovirus polyprotein (*16*).

p65 was immunoprecipitated specifically by UP102 and was not detected in mock-infected cells, nor by preimmune sera in MHV-A59-infected cells. Its size was consistent with the predicted gap in the model of ORF 1a expression and processing (1). p65 was first detected at 60 min of label, a delay of 30 min compared with p28. When the number of methionine plus cysteine residues in p28 and the predicted p65 domain (18 and 42 respectively) was considered, densitometric measurements of p28 and p65 indicated that up to 120 min was required for processing of amounts of p65 equivalent to p28. No intermediate precursor for p65 was detected in any experiments. The 81043 antibody was used as a control for immunoprecipitation of the cell lysates and detected an increasing amount of high-molecular-weight proteins beginning at 30 min, followed by the detection of p290 at 60 min (*1*). Molecular weight estimates were obtained as previously described with an accuracy within 10% for all proteins estimated (*1*). Together these data suggested a pattern of expression and processing at late times of infection in which p28 was rapidly cleaved from the growing polypeptide chain, followed by the delayed but concurrent cleavage of p65 and p290 from an elongating nascent polyprotein.

The pattern of p28 and p65 expression and cleavage was examined in more detail using two different types of pulse–chase experiments. In the variable-pulse/constant chase experiment, translation was synchronized in MHV-A59 cells with 200 m*M* NaCl, and the infected cells were then pulsed with [^{35}S]methionine for intervals of 5 to 90 min, followed by a 90-min chase (Fig. 3). This experiment allowed us to determine when during translation the proteins were labeled, since the chase allowed extensive processing of the products and the only variable was the length of labeling. In this experiment p28 and p65 were labeled within 15 min, which represented the earliest time that new protein products could be detected after high salt synchronization and addition of radiolabel. Thus both the antibody specificity and the time of labeling supported the conclusion that p65 was immediately adjacent to p28 in the polyprotein.

This early labeling of p65 was a distinct contrast to the time of cleavage of p65 in standard pulse–chase experiments. To assess the kinetics of cleavage, infected cells were pulse-labeled for 20 min followed by various chases ranging from 0 to 150 min (Fig. 4). It was possible to detect p28 at the end of the 20-min pulse period (0 min chase), whereas p65 was not detectable until 20 to 30 min of chase, and amounts of p65 equivalent to p28 by densitometry were not detectable until 90 min of chase. The amount of high-molecular-mass products detected by UP102 was stable until p65 began to appear and then decreased as p65 accumulated. This was consistent with immunoprecipitation of p65 as part of a larger polyprotein which was no longer detected once p65 was cleaved and supports the prediction that the high-molecular-mass products may be precursor polyproteins rather than nonspecific aggregates. Again, no intermediate precursors to p28 or p65 were identified despite the very

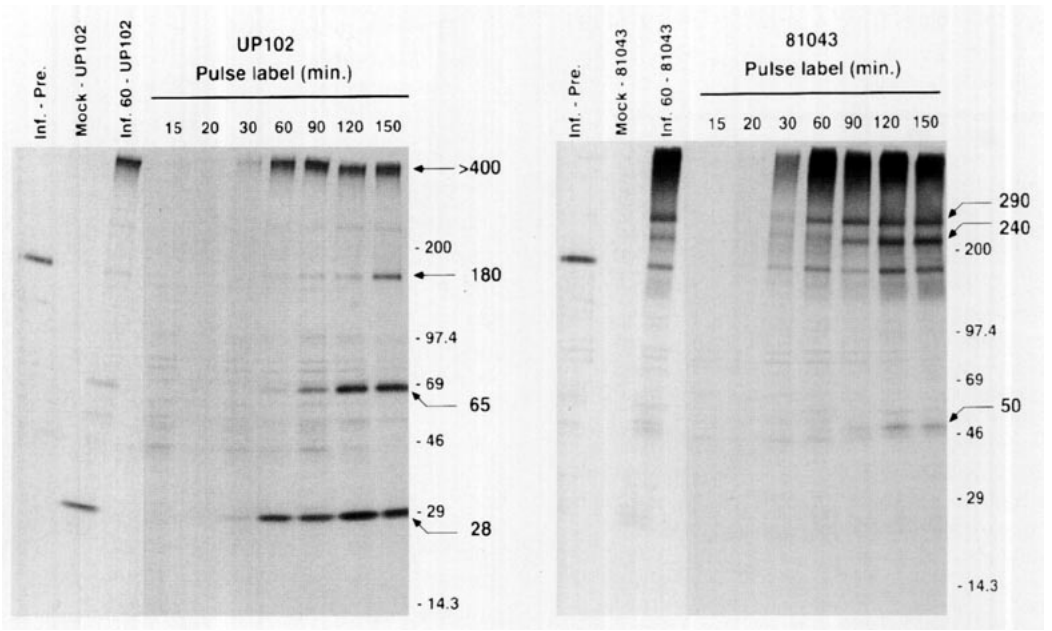

FIG. 2. Pulse-label translation of ORF 1a products in DBT cells following high salt synchronization. Monolayers of DBT cells were infected with MHV-A59 at an m.o.i. of 20 in DMEM 2% FCS. At 4 hr p.i., actinomycin D (10 μg/ml) was added to the medium. At 7 hr p.i., the medium was made hypertonic by the addition of NaCl at 200 m*M* in order to block reinitiation of translation and allow synchronization. At 7.5 hr p.i., the hypertonic medium was replaced with normal sodium medium containing 200 μCi/ml of [^{35}S]methionine. Cells were harvested at the times in minutes indicated. Cell lysates of 5×10^5 cells were immunoprecipitated with either antiserum UP102 or 81043 and products were subjected to electrophoresis in 5–18% gradient polyacrylamide gels. Inf.-Pre., infected cells radiolabeled for 60 min and immunoprecipitated with preimmune rabbit serum. Mock, mock-infected cells radiolabeled for 60 min and immunoprecipitated with respective antibodies. Inf. 60, infected cells labeled for 60 min in the absence of synchronization and immunoprecipitated with respective antibodies. Molecular mass markers are to the right of each gel preceded by dashes, and the estimated molecular masses of specific ORF 1a immunoprecipitation products are indicated by arrows.

early time points of chase used for assessment of cleavage, even on prolonged exposure of the gel.

p65 probably shares a cleavage site with p28 and thus is likely cleaved at its amino-terminus by the first papain-like proteinase (PLP-1) encoded in ORF 1a. The carboxy-terminal cleavage of p28 by PLP-1 occurs *in cis* during *in vitro* translation of RNA transcripts (*17, 2*). It is reasonable to postulate that the carboxy terminus of p65 is also cleaved *in cis* by PLP-1. *cis* cleavage of p65 would necessitate that PLP-1 was active within a much larger precursor protein, consistent with our observation that p65 appears to be cleaved from high-molecular-mass precursors without other intermediates. Such a mechanism of cleavage would also be consistent with the delayed appearance of p65, even at late times of infection. It has been suggested that all of the cleavages in the polyprotein encoded by the first 9.6 kb of gene 1 are effected by the two papain-like proteinases, since no sites compatible with cleavage by the predicted 3C-like proteinase have been identified in this region (*3, 5*). If this is the case, then the delayed cleavage of p65 compared to p28 suggests that cleavage of p28 may be an obligatory first step in the normal processing pathway of the gene 1 polyprotein. The carboxy-terminal cleavage sites of p65 may either be inaccessible until p28 is cleaved or may not be exposed until a larger polyprotein is expressed.

It has not been possible to study the expression and processing of p65 *in vitro*, since this polypeptide has not been detected during *in vitro* translation of either purified genome RNA or synthetic RNA transcripts encoding the first or second papain-like proteinase domain (*8, 18*). The maximum size product seen during translation of genome RNA, in the presence of proteinase inhibitors, is 250 kDa, and in the absence of proteinase inhibitors p28 is cleaved from this product. The remaining p220 may not be large enough to allow proper folding and proteinase/substrate interaction which would effect cleavage of p65.

Highly ordered patterns of expression and processing of the nonstructural polyprotein are seen in other RNA viruses, such as poliovirus, where cleavage of the P1 precursor occurs immediately after synthesis and before completion of the polyprotein, but processing of P1 into VP0, VP3, and VP1 is not achieved until the 3C or 3CD molecule is available (*19, 20*). Another interesting comparison is with the cowpea mosaic virus, a bipartite, plus-strand RNA virus which encodes polyproteins from both RNA segments. The larger B fragment is used to translate nonstructural proteins. The virus-encoded proteinase

cleaves an amino-terminal 32-kDa product as the initial, rapid, cotranslational event. This 32-kDa protein in turn regulates the rate of cleavage of the remaining 170 kDa of the polyprotein, including liberation of the 24-kDa proteinase itself (*21*). Although such a "chaperone" or bicomponent role has not been investigated for p28, the data obtained so far would not exclude such a role for p28 in the delayed generation of p65. Since our experiments were performed late in infection, it was not possible to determine whether cleavage of p65 was occurring *in cis*, *trans*, or both.

With the exception of the first papain-like proteinase, no activities have been demonstrated for any of the ORF 1a-encoded proteins. The region which encodes p65 does not possess any predicted replicase or proteinase functions and has no similarity to other cellular or viral proteins, and the predicted amino acid sequence in this region of MHV-A59 is not as highly conserved among coronaviruses as are other portions of gene 1. Experiments are currently underway to identify the amino- and carboxy-termini of p65, as well as to assess its exact relationship to p290. Recognition of the expression and processing of p65 in MHV-A59 will allow us to better assess the activities of the viral proteinases, as well as to investigate a protein which may possess functions unique in the replication strategies of plus-strand RNA viruses, and which may be diverged even among coronaviruses.

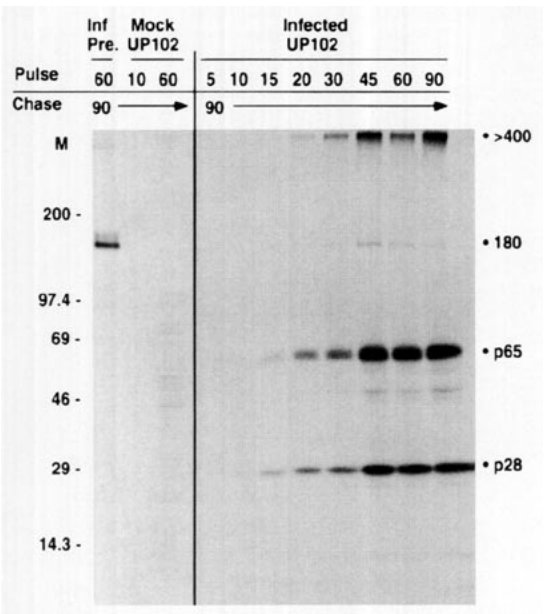

FIG. 3. Variable pulse–constant chase labeling of ORF 1a products. At 7.0 hr p.i. medium was made hypertonic by the addition of NaCl to 200 m*M*. At 7.5 hrs p.i., hypertonic medium was replaced with normal sodium media containing 200 μCi/ml of [^{35}S]methionine and 10 μg/ml of Actinomycin D for the indicated times ranging from 5 to 90 min. At each time point, the radiolabeled medium was removed from the plate and replaced with medium containing excess unlabeled L-methionine for an additional 90-min chase. At the end of the 90-min chase period, whole-cell lysates of 5 × 10^5 cells were immunoprecipitated with antiserum UP102 followed by electrophoresis on 5–18% gradient SDS–polyacrylamide gels. The duration of radiolabel prior to the 90-min chase is shown in the pulse lane. Inf Pre., infected cells immunoprecipitated by preimmune serum. Mock UP102, mock-infected cells immunoprecipitated with antiserum UP102. Molecular mass markers are to the left of the gel and locations of proteins immunoprecipitated by UP102 are to the right of the gel.

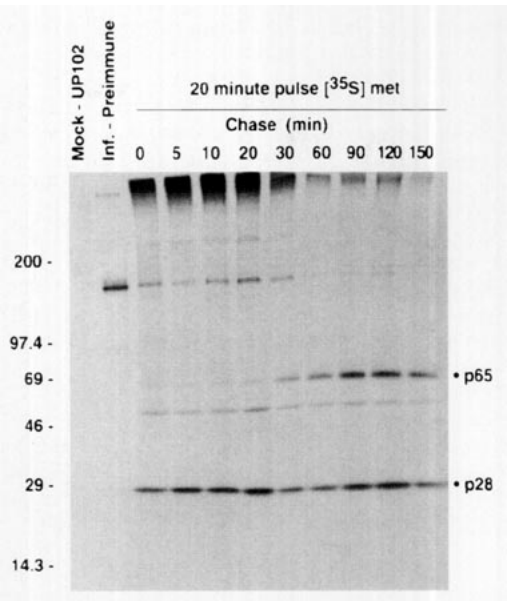

FIG. 4. Pulse–chase labeling of ORF 1a products in DBT cells. At 7.5 hr p.i., [^{35}S]methionine was added to the overlying medium for 20 min in the presence of 10 μg/ml of Actinomycin D, followed by a chase with excess unlabeled methionine for the times in minutes indicated. Whole cell lysates of 5 × 10^5 cells were immunoprecipitated with antiserum UP102 bound to protein A–Sepharose, and the products were analyzed on 5–18% gradient SDS–polyacrylamide gels. Molecular mass markers are to the left of the gel, and the locations of p65 and p28 proteins are indicated to the right of the gel. Mock-UP102, radiolabeled products of mock-infected cells labeled for 20 min and chased for 60 min. Inf.-Preimmune, radiolabeled products of infection labeled for 20 min, chased for 60 min, and immunoprecipitated with preimmune serum.

ACKNOWLEDGMENTS

We thank Philip Zoltick for construction of the UP102 expression construct and Bernadette Giangreco and Xiurong Wang for excellent technical assistance. This work was presented in part at the Fifth International Coronavirus Symposium, September 1992, and at the Third International Symposium on Positive Strand RNA Viruses, September 1992. This work was supported by Public Health Service Grants RO1 AI-26603 (MRD) and AI-17418 (SRW).

REFERENCES

1. Denison, M. R., Zoltick, P. W., Hughes, S. A., Giangreco, B., Olson, A. L., Perlman, S., Leibowitz, J. L., and Weiss, S. R., *Virology* **189,** 274–284 (1992).
2. Baker, S. C., Yokomori, K., Dong, S., Carlisle, R., Gorbalenya, A. E., Koonin, E. V., and Lai, M. M. C., *J. Virol.* **67,** 6056–6063 (1993).
3. Gorbalenya, A. E., Koonin, E. V., Donchenko, A. P., and Blinov, V. M., *Nucleic Acids Res.* **17,** 4847–4861 (1989).

4. Breedenbeek, P. J., Pachuk, C. J., Noten, A. F. H., Charite, J., Luytjes, W., Weiss, S. R., and Spaan, W. J. M., *Nucleic Acids Res.* **18,** 1825–1832 (1990).
5. Lee, H.-J., Shieh, C.-K., Gorbalenya, A. E., Koonin, E. V., LaMonica, N., Tuler, J., Bagdzhadhzyan, A., and Lai, M. M. C., *Virology* **180,** 567–582 (1991).
6. Bonilla, P., Gorbalenya, A., and Weiss, S., *Virology* **198,** 736–740 (1994).
7. Leibowitz, J. L., Weiss, S. R., Paavola, E., and Bond, C. W., *J. Virol.* **43,** 903–913 (1982).
8. Denison, M. R., and Perlman, S., *J. Virol.* **60,** 12–18 (1986).
9. Denison, M., and Perlman, S., *Virology* **157,** 565–568 (1987).
10. Denison, M. R., Zoltick, P. W., Leibowitz, J. L., Pachuk, C. J., and Weiss, S. R., *J. Virol.* **65,** 3076–3082 (1991).
11. Zoltick, P. W., Leibowitz, J. L., De Vries, J. R., Weinstock, G. M., and Weiss, S. R., *Gene* **85,** 413–420 (1989).
12. Hughes, S. A., Denison, M. R., Bonilla, P. J., Leibowitz, J. L., and Weiss, S. S., *In* "Coronaviruses: Molecular Biology and Virus–Host Interactions" (H. Laude and J.-F. Vautherot, Eds.), Vol. 342, pp. 221–226. Plenum Press, New York, 1993.
13. Pachuk, C. J., Breedenbeek, P. J., Zoltick, P. W., Spaan, W. J. M., and Weiss, S. R., *Virology* **171,** 141–148 (1989).
14. Saborio, J. L., Pong, S.-S., and Koch, G., *J. Mol. Biol.* **85,** 195–211 (1974).
15. Weiss, S., Hughes, S., Bonilla, P., Turner, J., Leibowitz, J., and Denison, M., *In* "Positive-Strand RNA Viruses" (M. Brinton, C. Calisher, and R. Rueckert, Eds.), Vol. 9(Suppl), pp. 349–358. Springer–Verlag, Vienna, Austria 1994.
16. Lawson, M. R., and Semler, B. L., *Virology* **191,** 309–320 (1992).
17. Baker, S. C., Shieh, C.-K., Soe, L. H., Chang, M.-F., Vannier, D. M., and Lai, M. M. C., *J. Virol.* **63,** 3693–3699 (1989).
18. Soe, L. H., Shieh, C.-K., Baker, S. C., Chang, M.-F., and Lai, M. M. C., *J. Virol.* **61,** 3968–3976 (1987).
19. Jore, J., de Geus, B., Jackson, R., Pouwels, P., and Enger-Valk, B., *J. Gen. Virol.* **69,** 1627–1636 (1988).
20. Dougherty, W. G., Parks, T. D., Cary, S. M., Bazan, J. F., and Fletterick, R. J., *Virology* **172,** 302–310 (1989).
21. Peters, S. A., Voorhorst, W. G. B., Wery, J., Wellink, J., and Van Kammen, A., *Virology* **191,** 81–89 (1992).